Cell Communication and Signaling

RESEARCH

Open Access

Polyoxometalate inhibition of SOX2-mediated tamoxifen resistance in breast cancer

Iskander Aurrekoetxea-Rodriguez[1], So Young Lee[1], Miriam Rábano[1], Isabel Gris-Cárdenas[1], Virginia Gamboa-Aldecoa[1], Irantzu Gorroño[1], Isabella Ramella-Gal[1], Connor Parry[1], Robert M. Kypta[1,2], Beñat Artetxe[3], Juan M. Gutierrez-Zorrilla[3] and Maria dM. Vivanco[1*]

Abstract

Background Increased cancer stem cell (CSC) content and SOX2 overexpression are common features in the development of resistance to therapy in hormone-dependent breast cancer, which remains an important clinical challenge. SOX2 has potential as biomarker of resistance to treatment and as therapeutic target, but targeting transcription factors is also challenging. Here, we examine the potential inhibitory effect of different polyoxometalate (POM) derivatives on SOX2 transcription factor in tamoxifen-resistant breast cancer cells.

Methods Various POM derivatives were synthesised and characterised by infrared spectra, powder X-ray diffraction pattern and nuclear magnetic resonance spectroscopy. Estrogen receptor (ER) positive breast cancer cells, and their counterparts, which have developed resistance to the hormone therapy tamoxifen, were treated with POMs and their consequences assessed by gel retardation and chromatin immunoprecipitation to determine SOX2 binding to DNA. Effects on proliferation, migration, invasion and tumorigenicity were monitored and quantified using microscopy, clone formation, transwell, wound healing assays, flow cytometry and in vivo chick chorioallantoic membrane (CAM) models. Generation of lentiviral stable gene silencing and gene knock-out using CRISPR-Cas9 genome editing were applied to validate the inhibitory effects of the selected POM. Cancer stem cell subpopulations were quantified by mammosphere formation assays, ALDEFLUOR activity and CD44/CD24 stainings. Flow cytometry and western blotting were used to measure reactive oxygen species (ROS) and apoptosis.

Results POMs blocked in vitro binding activity of endogenous SOX2. $[P_2W_{18}O_{62}]^{6-}$ (PW) Wells-Dawson-type anion was the most effective at inhibiting proliferation in various cell line models of tamoxifen resistance. 10 µM PW also reduced cancer cell migration and invasion, as well as SNAI2 expression levels. Treatment of tamoxifen-resistant cells with PW impaired tumour formation by reducing CSC content, in a SOX2-dependent manner, which led to stem cell depletion in vivo. Mechanistically, PW induced formation of reactive oxygen species (ROS) and inhibited Bcl-2, leading to the death of tamoxifen-resistant cells. PW-treated tamoxifen-resistant cells showed restored sensitivity to tamoxifen.

Conclusions Together, these observations highlight the potential use of PW as a SOX2 inhibitor and the therapeutic relevance of targeting SOX2 to treat tamoxifen-resistant breast cancer.

Keywords Breast cancer, Cancer stem cells, Resistance, Hormone therapy, SOX2 inhibition, Polyoxometalate

*Correspondence:
Maria dM. Vivanco
mdmvivanco@cicbiogune.es
[1]Cancer Heterogeneity Lab, CIC bioGUNE, BRTA, Technological Park Bizkaia, 801 A, Derio, Spain
[2]Department of Surgery and Cancer, Imperial College London, London W12 0NN, UK
[3]Department of Organic and Inorganic Chemistry, University of Basque Country UPV/EHU, Bilbao 48080, Spain

Background

Despite all the advances in research leading to improved therapies, breast cancer remains the first cause of death from cancer in women [1]. Around 75% of breast cancers express the estrogen receptor (ER) and are usually treated with hormone therapy, such as tamoxifen, an ER antagonist [2]. However, a 20-year follow-up meta-analysis has reported breast cancer risk of recurrence after stopping tamoxifen treatment can be up to 41% in some cases [3], highlighting the need for new approaches to reduce this risk.

Breast cancer is a heterogeneous disease. Inter-tumour heterogeneity (diversity among tumours from different patients) was clearly demonstrated by the identification of gene expression patterns that distinguish breast cancer subtypes correlated with patient outcome [4]. On the other hand, the existence of intra-tumour heterogeneity (complexity within a patient´s tumour) challenges therapy and management of breast cancer [5]. Breast tumours contain different cell types, including cells with stem cell features. A variety of methods that enrich for cells with characteristics of stem cells, as assayed by increased tumour initiation potential in transplantation studies, have shown the implication of cancer stem cells (CSCs) in tumour initiation and development of resistance to current forms of anti-cancer therapy [6, 7]. Our laboratory has demonstrated that resistance to endocrine therapy is driven by SOX2-mediated activation of CSCs [8, 9]. Tamoxifen treatment expanded different CSC sub-populations, including $CD44^{+}CD24^{-/low}$ cell population and cells with increased ALDEFLUOR activity and enhanced capacity to form mammospheres. Furthermore, high SOX2 levels were correlated with endocrine therapy failure in a cohort of ER-positive breast cancer patients treated with tamoxifen, highlighting the relevance of SOX family of transcription factors as potential therapeutic targets in breast cancer [8]. However, transcription factors are not easy to target, unless they are dependent on ligand activation as, for example, occurs with ER and other steroid hormone receptors [2].

Previous studies have identified the $K_6[P_2Mo_{18}O_{62}]$ Wells-Dawson-type polyoxometalate (POM) as a direct inhibitor of the SOX2-HMG domain produced in bacteria [10], suggesting the potential of these and other POMs against SOX factors [11]. Different members of this family of discrete and anionic metal oxo-clusters have been identified as promising inorganic drugs, that may act as antibacterial and antiviral agents [12] or to treat Alzheimer´s disease [13]. However, most biological studies to date have been devoted to their antitumor activity in multiple cancer types [14], including breast cancer cells [15], and they have shown potential to target cancer cells [14, 16, 17].

Therefore, we hypothesised that inhibition of SOX2 function by a POM would affect the CSC subpopulations and the sensitivity to tamoxifen. The main message of this work is that the combination of a traditional hormonal therapy with SOX2 inhibitors such as POMs may provide a novel approach to treat breast cancer. This strategy would reduce the risk of tumour recurrence. Considering the promising results reported in the literature for the direct inhibition of the SOX2-HMG domain produced in bacteria by POMs [10], herein we report on the first in vivo studies using three salts of anions with an identical negative charge: the commercial ammonium salt of the $[Mo_7O_{24}]^{6-}$ (Mo7) and two hydrated potassium salts of plenary Wells-Dawson-type heteropolyoxometalates, $[\alpha\text{-}P_2Mo_{18}O_{62}]^{6-}$ (PMo) and $[\alpha\text{-}P_2W_{18}O_{62}]^{6-}$ (PW).

To explore the potential of POMs to target SOX2 preferentially in CSCs, we compared the capacity of various POM derivatives to inhibit endogenous SOX2 DNA binding activity in breast cancer cells. The selected plenary Wells-Dawson type polyoxotungstate, PW, was found to be the most biologically active POM tested in a variety of functional assays. We show that treatment with PW results in the induction of apoptosis, particularly in cells with high SOX2 expression levels, reduction of the sizes of CSC subpopulations, and partial recovery of ER signalling, leading to impaired tumorigenicity of tamoxifen-resistant breast cancer cells in vivo. Therefore, the combination of tamoxifen (to target ER-positive breast cancer cells) and PW (to target SOX2-positive CSCs) could be a potential combinatorial treatment to treat breast cancer and reduce the risk of resistance to hormone therapy.

Methods

Synthesis of polyoxometalate salts

Compounds $K_6[\alpha\text{-}P_2Mo_{18}O_{62}]\cdot 12H_2O$ (where PMo = $[\alpha\text{-}P_2Mo_{18}O_{62}]^{6-}$) $K_6[\alpha\text{-}P_2W_{18}O_{62}]\cdot 14H_2O$ (where PW = $[\alpha\text{-}P_2W_{18}O_{62}]^{6-}$) were prepared following previously reported procedures with minor modifications [16], which imply the combination of the heteroatomic and addenda-metal source in acidic aqueous media under reflux conditions, followed by two purification cycles by recrystallization. Briefly, for PMo, a mixture of 20 g of $Na_2MoO_4\cdot 2H_2O$ (Sigma-Aldrich, ACS reagent > 99%, 0.082 mol), 3 mL of 85% H_3PO_4 (0.044 mol) and 16.5 mL of HCl (36.5–38.0% Sigma-Aldrich, BioReagent, 0.201 mol) in 50 mL of water was refluxed for 8 h. Then, the solution was cooled down to room temperature and a pale-yellow salt was precipitated by the addition of 20 g of KCl. This mixture was kept at 5 °C overnight, and the yellow solid was filtered and dried under vacuum. The crude product was purified by recrystallization in water. Yield: 9.5 g (64% based on Mo). FTIR, ν (KBr, cm^{-1}):

1076(s), 1003(w), 941(s), 905(s), 779(s). ^{31}P-NMR δ (D_2O, ppm): -3.00.

For PW, a mixture of 50 g of $Na_2WO_4{\cdot}2H_2O$ (Sigma-Aldrich, BioUltra > 99.0%, 0.15 mol) and 40 mL of 85% H_3PO_4 (Sigma-Aldrich, BioUltra, 0.60 mol) in 100 mL of water was refluxed for 4 h. Then, the solution was cooled down to room temperature and a pale-yellow salt was precipitated by the addition of 20 g of NH_4Cl (Sigma-Aldrich, ACS reagent > 99.5%). This product was collected and re-dissolved in 50 mL of warm water with 5 g of NH_4Cl. Afterwards, the potassium salt was precipitated from the cold solution with 8 g of KCl (Sigma-Aldrich, AC Reagent > 99%). This solid was collected, dissolved in 50 mL of hot water and kept at 15 °C overnight. Then, white needles of $K_{14}Na[P_5W_{30}O_{110}]{\cdot}nH_2O$ that could appear during this period were removed and the clear solution was refluxed for 6 h. A polycrystalline pale green solid was precipitated from the cold solution with 8 g of KCl. This solid was filtered, purified by recrystallization in water (pH = 2) and dried under vacuum. Yield: 16.7 g (41% based on W). FTIR, ν (KBr, cm^{-1}): 1091(s), 962(s), 914(s), 787(s). ^{31}P-NMR δ (D_2O, ppm): -12.89.

The stepwise synthesis of the fluorescent hybrid POM salt $TBA_6K[\alpha_2\text{-}P_2W_{17}O_{61}\{Sn(CH_2)_2CONHC_{20}H_{11}O_5\}]$ (where PW-F = $[\alpha_2\text{-}P_2W_{17}O_{61}\{Sn(CH_2)_2CONHC_{20}H_{11}O_5\}]^{7-}$) was carried out as previously reported [18]. All other reagents, including the ammonium heptamolybdate $(NH_4)_6[Mo_7O_{24}]{\cdot}4H_2O$ (where Mo7 = $[Mo_7O_{24}]^{6-}$; Sigma-Aldrich, ACS reagent, 99.98%, CAS 12054-85-2), were purchased from commercial sources and used without further purification.

POM characterisation

Infrared spectra (FT-IR) were recorded as KBr pellet on a Shimadzu FTIR-8400 S spectrophotometer in the 400–4000 cm^{-1} spectral range. UV/Vis spectra were registered on a Shimadzu UV mini 1240 spectrophotometer for samples dissolved in DMEM (8% FBS), whereas fluorescence emission spectra were acquired in an Edinburgh Instruments F980 fluorimeter using a continuous Kimmon Koha IK-Series HeCd laser (325 nm) as excitation source. Powder X-ray diffraction (PXRD) pattern was recorded from 2θ = 5 to 38° (0.038 step size, 30 s per step) using a Philips X'PERT PRO diffractometer operating at 40 kV/40 mA in θ–θ configuration with monochromated CuKα radiation (λ = 1.5418 Å) and a PIXcel detector. Nuclear magnetic resonance ^{1}H- and proton decoupled ^{31}P-NMR spectra were recorded on a Bruker Avance 500 MHz instrument for samples dissolved in D_2O, DMEM (8% FBS) supplemented with D_2O or CD_3CN (for PW-F). Chemical shifts (δ) are reported in parts per million (ppm) and referenced to TMS and 85% phosphoric acid for ^{1}H- and ^{31}P-NMR, respectively.

Culture of human cell lines

The ER-positive breast cancer cell lines MCF7, T47D and ZR75-1, were obtained from the American Tissue Culture Collection (ATCC), as well as human embryonic kidney HEK-293T cells (isolated from the kidney of a human embryo, CRL-3216, ATCC). All cell lines were cultured at 37 °C and 5% CO_2 in DMEM (Gibco, cat nr. 41965-039), 8% FBS (Fetal Bovine Serum Gibco™, 10270-106) 1% P/S (Penicillin/streptomycin, Gibco™, 1015140-122). DNA profiling (Eurofins Genomics, Germany) authenticated cell lines were routinely tested for mycoplasma. The control, parental cell lines are referred to as MCF7c, T47Dc, ZR75-1c and the corresponding tamoxifen-resistant breast cancer cell lines, MCF7TamR, T47DTamR and ZR75-1TamR, were developed in the laboratory after long-term (over 6 months) exposure to 5×10^{-7} M 4-Hydroxytamoxifen, referred herein as tamoxifen (Sigma, cat nr. H7904), as previously described [8]. Tamoxifen-resistant cells were maintained in culture in the presence of 5×10^{-7} M tamoxifen, while control cells were grown in presence of ethanol (vehicle).

The POMs were dissolved in culture medium to generate 2 mM stock solutions, which were used at the concentrations indicated in the figures. PW was used at a final concentration of 10 μM, unless otherwise indicated. The colour of the culture medium, which contains phenol red as a pH indicator, was not altered by addition of the POMs, reflecting that the solution remained at physiological pH. The aqueous solutions for ^{31}P-NMR studies were either colourless (Mo7 or PW) or yellow (PMo), indicating the absence of reduced blue species.

Electrophoresis mobility shift assay (EMSA)

Lentiviral expression plasmids pSin-EF2-Sox2-Pur (plasmid nr. 16577, Addgene, to express Homo sapiens SRY (sex determining region Y)-box 2, SOX2) and pSin-EF2-EGFP-Pur (as control, previously generated by our lab [19] in order express the jellyfish green fluorescent protein GFP) were transfected into HEK-293T cells (isolated from the kidney of a human embryo, CRL-3216, ATCC) to enrich for human SOX2 in protein extracts. Nuclear protein fractions were collected, as described [20]. EMSA was performed using double-stranded DNA (dsDNA) probe synthesized to contain the predicted SOX2 binding site in the promoter of the *P21* gene (human cyclin dependent kinase inhibitor 1A, *CDKN1A*, gene ID: 1026) and a sequence of the *PAX6* gene (human paired box gene 6, gene ID: 5080) promoter as negative control [11]. dsDNA sequences for the *P21* gene promoter sequences F: 5'- GGCCTCAAGATGCTTTGTTGGGGTGTCTA G-3' and R: 5'- CTAGACACCCCAACAAAGCATCTTG

AGGCC-3' and for the *PAX6* gene F: 5'- AAGCATTTTC ACGCATGAGTGCACAG-3' and R: 5'- CTGTGCACTC ATGCGTGAAAATGCTT-3'. Then, nuclear extracts were incubated in 20 mM HEPES, 5 mM $MgCl_2$, 10 mM KCl, 5% glycerol, 0.2 mM EDTA, 1 mM DTT, 1X protease inhibitor, for 30 min in the presence or absence of POM anions to allow binding to SOX2 protein. After that, dsDNA oligomers were added to the mixture at 1 mM concentration for further 60 min incubation at RT. Protein-DNA complexes were separated in native gels and for DNA staining after electrophoresis, gels were incubated in 20 mL of 0.5X TAE buffer and 2 µL of GelRed® Nucleic Acid Gel Stain (Biotium) for 20 min at RT. Pictures were taken in an ultraviolet transilluminator.

Chromatin immunoprecipitation (ChIP)

SimpleChIP® Enzymatic Chromatin IP Kit commercial kit from Cell Signaling was used. Briefly, 10^7 cells were cross-linked with 1% formaldehyde and the reaction was quenched by 1 M glycine, followed by cell lysis with the provided buffers. Subsequently, nuclei were digested by the addition of Micrococcal nuclease for 20 minutes at 37°C in an orbital shaker. The reaction was quenched by the addition of 0.05 M EDTA. Micrococcal nuclease digestion was followed by sonication to shear chromatin. Chromatin was subjected to RNAse and Proteinase K treatment followed by DNA purification. At this point, 2% of the purified chromatin was removed as input control. Chromatin was incubated at 4°C overnight in rotation with either control rabbit IgG or SOX2 antibody (Cell Signaling, mAb#3579). Eluted and input chromatin were purified and subjected to qPCR analysis. All ChIP analyses were performed as triplicate technical repeats for each of three independent experiments and analysed following the percent input method. *P21* gene (human cyclin dependent kinase inhibitor 1A, *CDKN1A*, gene ID: 1026) was analysed with the primers: F: 5'- CTGTTTC CCTGGAGATCAGGT −3' and R: 5'- ACTGATCCCTC ACTAGGTCAC −3'. *CCND1* gene (Cyclin D1, gene ID: 595) was analysed with the primers: F: 5'- TGCCGGGC TTTGATCTTT −3' and R: 5'- CGGTCGTTGAGGAGG TTGG −3'.

Cell proliferation and spheroid formation assays

To evaluate POM effects on cell proliferation, 5,000 cells/well were seeded in culture medium in 24-well tissue-culture plates. POM treatments were freshly prepared every time. Cell proliferation was determined after 7 days by staining cells with crystal violet solution (Sigma, cat nr. C0775). Briefly, cells were washed twice with PBS and fixed with 200 µL of 4% PFA for 15 min before staining with 200 µL of crystal violet for 20 min on a rocker to ensure all the surface was covered. Then, cells were washed twice with PBS and plates allowed to dry overnight. Stained cells were dissolved in 10% acetic acid solution and absorbance was measured at 595 nm. Results are shown as relative cell proliferation to the control using the mean of three independent experiments.

Spheroid formation assays were performed as previously described [21]. Briefly, five thousand cells were seeded per well in 96-well ultra-low-attachment plates (Corning, cat nr. 3474) and spheroids allowed to form in the absence or presence of 10 µM PW. Matrigel growth factor reduced (BD, cat nr. 354230) was added on the top of the spheroids, and their growth and cell invasion were monitored. The invaded area was quantified using ImageJ software.

RNA extraction, quantitative real-time PCR and western blotting

Total RNA was extracted using the illustra™ RNAspin Mini Isolation Kit (GE Healthcare) following the manufacturer's instructions. Total RNA was used for reverse transcription using the M-MLV Reverse Transcriptase and RNase OUT Ribonuclease Inhibitor (Invitrogen), according to manufacturer's instructions. qPCR was performed using PerfeCTa SYBR® Green Supermix, Low Rox (Quanta Biosciences) in either a Viia7 or QuantStudio 6 Flex Real-Time PCR System (Applied Biosystems). Relative levels of mRNA were determined according to the ΔΔCT quantification method, relative to the housekeeping gene 36B4. The primers used for qPCR amplification are listed in the Supplementary materials and methods.

Western blotting was performed as previously described [9]. Blots were incubated with the following primary antibodies: rabbit anti-Parp (Cell Signaling, cat nr. 9542), mouse anti-Bcl-2 (EMD Millipore, cat nr. OP60-20UG) and mouse anti-b-actin (Sigma, cat nr. A5441). For detection, an enhanced chemiluminescence detection kit (Clarity Western ECL Substrate, Bio-Rad, cat nr. 1705061) was used.

Migration and invasion assays

Migration (wound healing) assays were performed by growing cells to confluency and a thin wound produced by scratching with a pipette tip. Migration into the wounded space was quantified using ImageJ. Invasion assays were performed in a 24-well Corning BioCoat Matrigel® Invasion Chambers (Corning, cat nr. 354480) containing an 8 µm pore size PET (PolyEthyleneTerephthalate) membrane, as previously described [22]. Briefly, 50,000 MCF7TamR cells/well, previously starved in medium with 1% FBS, were seeded in triplicate and 20% FBS containing medium was added to the wells below, both in presence or absence of PW treatment. As a control for cell viability, cells were plated in parallel at the same density in 24-well tissue culture plates. After 72 h, invaded cells were fixed and stained with crystal violet

solution and at least 9 different fields of each well were counted using ImageJ software. Results are shown as relative cell invasion of three independent experiments.

Generation of stable gene silencing and gene knock-out using CRISPR-Cas9 genome editing technology

The 3-plasmid transfection system was used for the lentiviral stable knockdown of *SOX2* gene, using pLKO.1 backbone vector. pLKO.1-shSOX2 was used against *SOX2* gene and an empty shRNA vector (pLKO.1-empty) was used as negative control. The protocol for lentivirus infection was performed in several steps as previously described [19].

CRISPR-Cas9 targeting of *SOX2* locus was performed using online resources (CRISPRdesign and CRISPR) to search for high-scoring sites in the *SOX2* gene locus. The highest scoring sgRNA target to design the vectors were chosen and cloned into the nickase plasmid pSpCas9(BB)-2A-Puro (PX459) V2.0. sgRNA oligo sequences were: sgRNA A, 5'-CACCGCTCCATCATG TTGTACATGC-3' and B 5'- CACCGCGGGCCCGCA GCAAACTTCG-3'. All constructs were confirmed by sequencing and cloning. MCF7TamR cells were transiently transfected with the resulting CRISPR-Cas9 vector together with one (as control) or both sgRNA sequences against *SOX2* gene locus, using GeneJuice® Transfection Reagent. Two days after transfection, transfected cells were selected with 2 μg/mL puromycin and followed by single cell cloning and screening. The efficiency of stable Sox2 knockout was confirmed by western blotting, resulting in a depleted Sox2 cell line (MCF7TamR-Sox2KO).

CSC assays

For CD44/CD24 stainings, the same protocol as previously described was used [8]. Briefly, cells were labelled with PE-conjugated mouse anti-CD24 antibody (BD, ML5/BD, 555428) and APC-conjugated mouse anti-CD44 antibody (BD, G44-26/BD, 559942) and incubated for 30 min on ice with the respective antibodies diluted in 1% BSA in PBS. Control cells were stained with isotype-matched control antibodies. The cell viability dye 7AAD (BD) was added for dead cell exclusion.

For mammosphere cultures, cells were detached with TrypLE 1X (Invitrogen, 12604021) and plated in ultralow attachment 24-well tissue-culture plates (Corning, cat nr. 3473) at a density of 500 cells/well, as previously reported [9]. To assess the self-renewal capacity of stem cells, primary mammospheres (I MS) were dissociated with TrypLE 1X after 5 days to obtain a single-cell suspension and seeded to produce a new generation of secondary mammospheres (II MS). The number of mammospheres was calculated as the average of 4 wells for each cell line in at least three independent experiments.

The ALDEFLUOR assay was performed following the manufacturer guidelines (STEMCELL Technologies, cat nr. 01700) using 10^6 cells/sample. DRAQ7 (Thermo Fisher, cat nr. D15105) dye was used to measure the viability of the cells and exclude dead cells. Control tubes were always used to ensure accurate gating for ALDH negative activity, adjusting FCS (Forward Scatter) and SSC (Side Scatter) voltages according to cell size and complexity. Samples were run in a FACSAria cytometer and data were analysed using the FACSDiva software.

Tumour growth assay on the CAM

Chick embryo chorioallantoic membrane (CAM) assays were performed as previously reported [23]. Briefly, separation of the developing CAM was induced on embryo development day 4, EDD4, by cutting a 2 mm diameter hole at the sharp end. At EDD7, 500,000 MCF7TamR-GFP cells/egg (unless otherwise indicated, like in the ELDA assays) were implanted. At EDD10, eggs were placed on ice for 1 h to anaesthetise the embryos, and tumours were photographed in vivo and excised. Tumour specimens were excised from the CAM and cells dissociated using collagenase (Sigma, cat nr. CO130). DRAQ7 dye was used to measure cell viability and the number of GFP+cells quantified using a FACSCanto cytometer. Data were analysed using the FACSDiva software.

ROS assay

Mitochondrial ROS was quantified by flow cytometry, following the recommendations of the manufacturer. Briefly, 350,000 MCF7c and MCF7TamR cells were plated in 6-well plates. Cells were grown in the presence or absence of either 10 or 20 μM PW for 48 h before staining them with 2.5 μM MitoSOX (Thermo Fisher, cat nr. M36008) during 30 min at 37°C in PBS with Ca^{2+} and Mg^{2+}, following manufacturer's instructions. FACS gatings were established with unstained control cells and the percentage of cells positive to the probe was analysed and presented as fold change.

Apoptosis assay

Annexin V staining was performed as previously described [24] and using FITC Annexin V Apoptosis Detection kit (BD, 556547), following the instructions of the manufacturer and using DRAQ7 for cell viability. Cells were analysed using FACSAria (BD) flow cytometer and the FACSDiva software.

Transient transfection and transcriptional assay

ER transcriptional activity was analysed as previously described [8]. Briefly, cells were seeded in 24-well plates at 50,000 cells/well and grown in charcoal-treated conditions for 24 h. The cells were transfected with the ERE-TK-luciferase reporter and pRL β-galactosidase

[20] to normalise for transfection efficiency, using Lipofectamine LTX with Plus reagent (ThermoFisher Scientific, cat nr. 15338100) following the manufacturer´s instructions. After transfection, the cells were maintained in phenol red free medium containing 8% charcoal-stripped FBS treated with 10^{-8} M estrogen or 5×10^{-7} M tamoxifen or ethanol (vehicle) for 72 h. For experiments combining tamoxifen and estrogen (Fig. S6A-C), both hormones were used at equimolar concentrations, both at 10^{-7} M. The cell lysates were assayed for luciferase and β-galactosidase activities using the Luciferase assays kit (Promega, E1501) and the Galacto-Light™ (ThermoFisher Scientific, cat nr. T1055) with Galacton-Plus™ Substrate (ThermoFisher Scientific, T2120), respectively, according to the instructions of the manufacturers and using a luminometer (Turner Biosystems). The luciferase results are shown as relative light units of luciferase activity normalised with respect to β-galactosidase activity.

Statistical analysis

Data from at least three independent experiments were expressed as means +/- standard deviation, SD. Each data point of qPCR, mammosphere formation, luciferase activity, proliferation, CAM and invasion assays were run at least in triplicates and independent experiments were performed at least three times. Student´s *t*-test or ANOVA were used to determine statistically significant differences and $p<0.05$ was considered to be statistically significant unless otherwise specified.

Results

POMs inhibit SOX2 DNA binding activity

We wished to explore the potential of polyoxometalates (POMs) to inhibit SOX2 in breast cancer cells. To this end, we used MCF7 cells, a well-known ER-positive breast cancer cell line, and MCF7TamR cells as a model of resistance to tamoxifen previously developed in the laboratory that express high levels of SOX2 [8]. We analysed POMs that have been shown to inhibit the DNA binding activity of SOX2 [10] and other SOX-HMG family members [11]. The majority of SOX factors exhibited downregulation, absence of expression or minimal detectability in MCF7 breast cancer cells, and only SOX2 and SOX9 were upregulated in tamoxifen-resistant MCF7TamR cells, although SOX2 demonstrated a greater fold increase from parental to resistant cells than SOX9 (Fig. S1A). In fact, SOX2 levels were the highest also in other two cell models of resistance to tamoxifen developed from the ER-positive cell lines T47D and ZR75-1, T47DTamR and ZR75-1TamR, respectively [8]. Thus, we focused on analysing the potential inhibitory effects of POMs on SOX2 activity.

Three different POM salts were tested (Fig. 1A): the commercial ammonium salt of the $[Mo_7O_{24}]^{6-}$ (Mo7) anion [25], an isopolyoxomolybdate shown to display antitumoral activity against several cancer cell types [25, 26], and two hydrated potassium salts of Wells-Dawson-type heteropolyoxometalates, $[\alpha\text{-}P_2Mo_{18}O_{62}]^{6-}$ (PMo) and $[\alpha\text{-}P_2W_{18}O_{62}]^{6-}$ (PW), synthesised following reported procedures [16] and previously shown to inhibit the interaction of the purified SOX2-HMG domain to short DNA sequences in vitro [10, 11]. Infrared spectroscopy (FT-IR) and ^{31}P-NMR confirmed the identity and purity of PMo and PW [16, 27] (Fig. S1B). Furthermore, powder X ray diffraction (PXRD) analyses indicated the phase homogeneity of $K_6[\alpha\text{-}P_2W_{18}O_{62}]\cdot14H_2O$, with experimental profiles virtually identical to those calculated from single-crystal X-ray diffraction data (ICSD-24673) (Fig. S1C).

Gel retardation assays showed that SOX2 binding to specific DNA sequences from the p21 (*CDKN1A*) promoter, a recognised SOX2 target, was completely inhibited by 10 μM PW, while 50 μM PMo was required to obtain a similar effect, and Mo7 failed to reduce SOX2 binding in vitro (Fig. 1B). In contrast, GFP overexpression (Fig. S1D) or incubation with non-specific DNA sequences from the *PAX6* gene, lacking SOX2 binding sites [11] did not form any protein/DNA complexes (Fig. S1D). These experiments suggest the potential of POMs to inhibit full-length SOX2 DNA binding activity and, in particular, of PW, which can be modelled interacting with the positively charged SOX2 DNA binding domain (Fig. 1C).

Cell viability dose-dependent curve assays were performed using MCF7c, MCF7TamR and MCF7 cells overexpressing SOX2 (MCF7Sox2) [19]. PW reduced cell viability at lower concentrations than Mo7 and PMo (Fig. S1E). The ^{31}P-NMR spectrum of PW in deuterated water (D_2O) exhibited one singlet at $\delta = -12.89$ ppm [28] and was comparable with that recorded in cell culture medium (Fig. 1D), even after one week (Fig. 1E). In contrast, PMo is relatively stable in culture medium, but it undergoes a partial dissociation process to Keggin-type lacunary species in one day (Fig. S1F), as previously reported [28]. This observation can partly explain its lower inhibitory activity in comparison to that of PW. These analyses confirmed the stability of PW in biological cell culture media and were ratified by electrospray ionization mass spectrometry (ESI-MS) analysis (Fig. S1G).

To determine the intracellular localisation of PW in culture, the related $[\alpha_2\text{-}P_2W_{17}O_{61}]^{8-}$ α_2-Wells-Dawson monolacunary derivative was functionalised with an organotin group, following reported procedures [18]. The subsequent EEDQ-activated coupling of the organic ligand bearing a carboxylic acid residue with a fluorescein amine through amide bond formation resulted in the hybrid POM $[\alpha_2\text{-}P_2W_{17}O_{61}\{Sn(CH_2)_2CONHC_{20}H_{11}O_5\}]^{7-}$ (PW-F). The success of this synthesis and the stability of

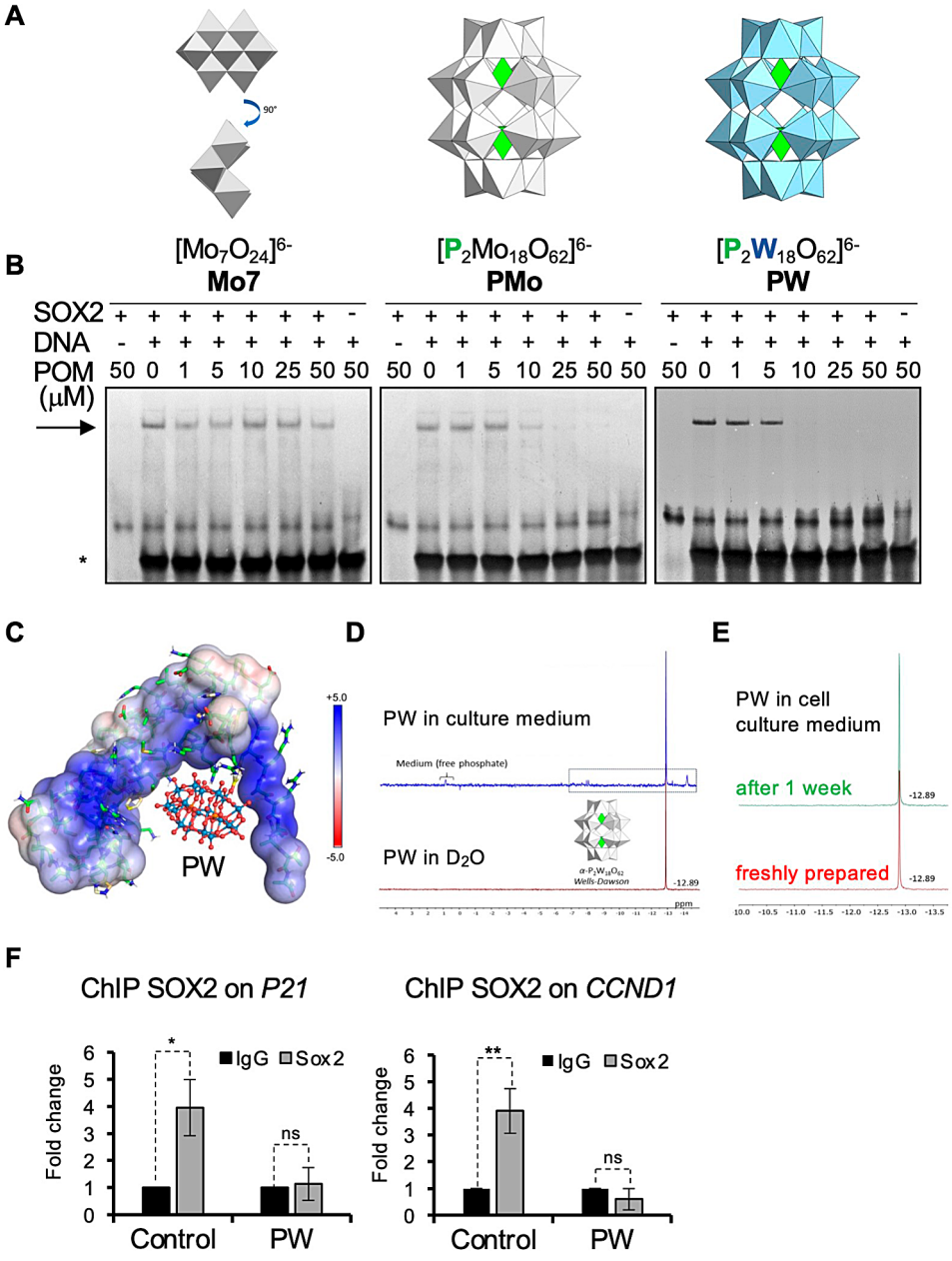

Fig. 1 POM inhibition of SOX2 binding to DNA. (**A**) Molecular species of Mo7, PMo and PW anions. (**B**) *P21* site DNA binding of SOX2 from HEK-293T nuclear extracts, incubated with increasing concentrations of POM anions, by mobility shift assays. The arrow indicates protein/DNA complex and the asterisk free DNA. (**C**) Model of interaction between SOX2 DNA binding domain and PW constructed considering the electrostatic surface of the biomolecule using APBS plugin, as incorporated in the PyMOL software package. (**D**) ^{31}P-NMR spectrum of PW in deuterated water (D_2O) (bottom) and in cell culture medium (top). Inset: Expanded – 7.00 to 14.5 ppm region. Resonance at -12.89 ppm corresponds to the [α-$P_2W_{18}O_{62}$]$^{6-}$ Wells-Dawson anion. Low intensity signals have been tentatively assigned to: (a) [α_2-$P_2W_{17}O_{61}$]$^{8-}$, (b) [$H_2P_2W_{12}O_{48}$]$^{12-}$ and (c) [α-$PW_{12}O_{40}$]$^{3-}$. (**E**) ^{31}P-NMR spectra of PW in freshly prepared cell culture medium or after one week. (**F**) Chromatin immunoprecipitation of SOX2 on *P21* and *CCND1* promoters in MCF7TamR cells in the absence or presence of 10 μM PW; IgG was used as antibody control. Graphs represent mean and standard deviation of three independent experiments; *p* values (*$p < 0.05$, **$p < 0.01$) were calculated using two-tailed Student´s *t*-test, ns indicates not significant

the hybrid species in solution was confirmed by a combination of FTIR, UV-Vis, ^{1}H-NMR and fluorescence emission spectroscopies (Fig. S1H, S1I).

Immunofluorescence analysis confirmed entry of PW-F into cells and its nuclear localisation, both at 24 h and 48 h (Fig. S1J). Furthermore, chromatin immunoprecipitation showed that PW inhibited specific SOX2 binding to two recognised target regions of the p21 (*CDKN1A*) and cyclin D1 (*CCND1*) promoters (Fig. 1F). Together, these results confirm the specific inhibition of endogenous SOX2 binding to DNA by PW in cultures of tamoxifen-resistant cells.

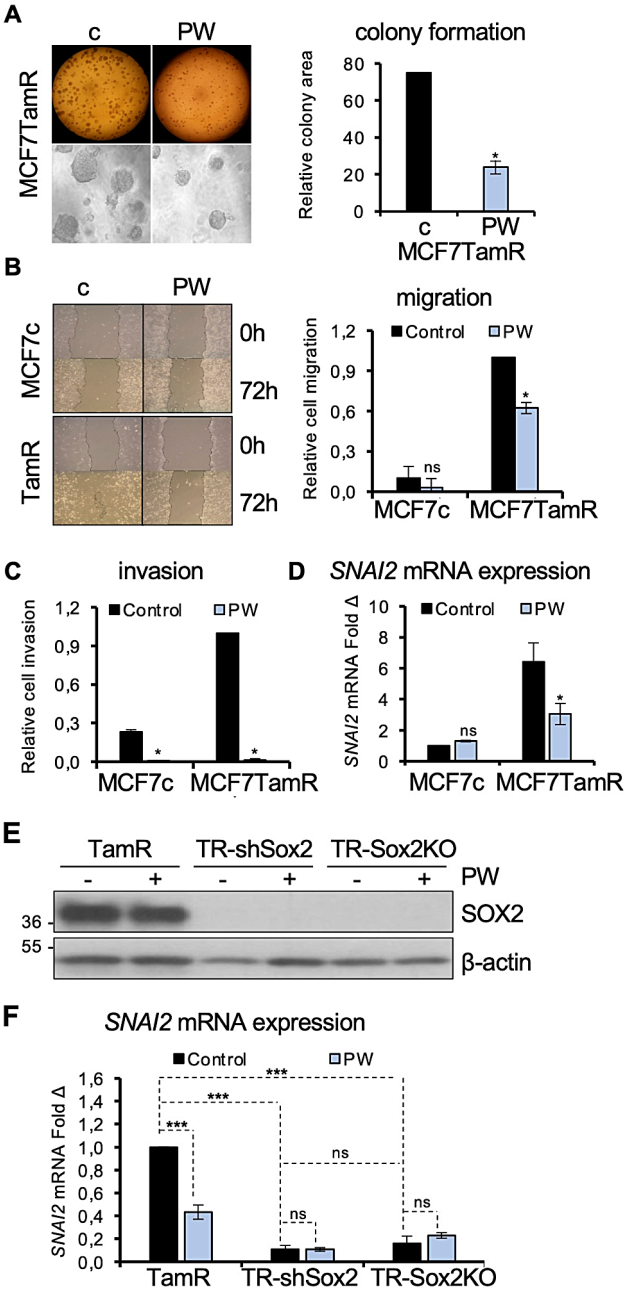

Fig. 2 Effects of PW on breast cancer cells. (**A**) Representative images of MCF7TamR spheroids grown in Matrigel in the absence (carrier control, c) or presence of 10 μM PW for 7 days (left; bottom is a magnification of top images) and colony area quantification (right). (**B**) Typical images of wound healing assay for cell migration of MCF7 control (MCF7c) and MCF7TamR cells (left) and (right) quantification calculated as area occupied by cells at 72 h culture versus at 0 h, in response to 10 μM PW. (**C**) Matrigel invasion assay was performed using MCF7c and MCF7TamR cells in the presence or absence of 10 μM PW. (**D**) Transcript levels of *SNAI2* in control and tamoxifen resistant cells cultured in the absence (control) or presence of 10 μM PW. (**E**) Representative images of immunoblot analysis for SOX2, and β-actin as loading control, in MCF7TamR, MCF7TR-shSox2, MCF7TR-Sox2KO cells. (**F**) *SNAI2* mRNA levels after treatment with 10 μM PW for 72 h (PW) in MCF7TamR, MCF7TR-shSox2 and MCF7TR-Sox2KO cells. In all cases ($n = 3$). Error bars represent standard deviation, p value: $^{*}p < 0.05$

PW reduces aggressiveness of tamoxifen-resistant breast cancer cells

Cell proliferation in response to PMo or PW was compared using three different breast cancer models of resistance to tamoxifen, MCF7TamR, T47DTamR and ZR75-1TamR cells [8] with the concentration of POM capable of fully disrupting SOX2-DNA complexes in vitro (50 μM PMo and 10 μM PW). PMo displayed similar effects in all cells, both control and resistant (Fig. S2A), whereas PW significantly compromised viability of tamoxifen-resistant cells in both 2D (Fig. S2B) and 3D (Fig. 2A) for all three cell models of resistance. PW reduces cell viability also in the absence of tamoxifen in tamoxifen resistant cells, however the reduction was strongest in all resistant cells when PW was combined with tamoxifen (Fig. S2C). These findings suggest that PW inhibition of SOX2 transcriptional activity renders tamoxifen-resistant cells more sensitive to tamoxifen in vitro.

Cells resistant to tamoxifen and with high SOX2 expression levels exhibit increased migration and invasion capacities [8], thus we hypothesised that PW treatment might inhibit these processes. Wound healing assays showed that the increased cell migration capacity of tamoxifen-resistant cells was significantly reduced by 40% by PW treatment (Fig. 2B). Moreover, analysis of invasion capacity through Matrigel revealed significant inhibition of cell invasion by PW treatment in both resistant and control cells, although the invasion capacity was 4.5-fold stronger in tamoxifen-resistant cells (Fig. 2C).

Upregulation of SOX2 expression has been shown to lead to SLUG/SNAI2 induction, promotion of epithelial to mesenchymal transition (EMT) and increased cancer cell invasion and metastasis [29]. Furthermore, SNAI2 has also been found in human luminal progenitors [9] and its high expression in breast cancer metastasis has been correlated with shorter progression-free survival of patients on endocrine therapy [30]. Analysis of *SNAI2* mRNA expression demonstrated increased levels in tamoxifen-resistant cells, which were significantly reduced by over 50% by PW treatment (Fig. 2D). To determine to what extent this effect was a consequence of PW-mediated inhibition of SOX2, we generated MCF7TamR cells with knock-down expression of SOX2 by stable silencing using specific short-hairpin RNA sequences (TamR-shSox2) or by deletion of endogenous SOX2 using CRISPR-Cas9 technology (TamR-Sox2 KO) (Fig. 2E). Tamoxifen-resistant cells lacking SOX2 expression showed over 85% reduction in *SNAI2* expression levels and PW treatment did not further reduce this effect (Fig. 2F). These findings suggest that PW treatment reduces SOX2-dependent SNAI2 expression, contributing to the inhibition of migration and invasion in tamoxifen-resistant cells.

PW impairs tumorigenicity of tamoxifen-resistant cells in vivo

We have previously shown that tamoxifen-resistant cells are more tumorigenic than parental control cells and that overexpression of SOX2 enhances resistance to the anti-proliferative effects of tamoxifen treatment in vivo [8]. To explore whether inhibition of SOX2 activity by PW treatment affects tumour progression in vivo, we used the chick embryo chorioallantoic membrane (CAM) model, which provides cell explants with a blood supply delivering nutrients and growth factors and that has been established as a useful experimental system to study tumour biology [31, 32]. To enable quantification of tumour cell growth, we generated a stable tamoxifen-resistant cell line overexpressing GFP protein (MCF7TamR-GFP cells). MCF7TamR-GFP cells were grafted onto the exposed CAM of chicken embryos in the presence or absence of two different concentrations of PW (10 or 20 μM PW). Quantification of GFP-positive cells showed a significant reduction in the size of tumours arising from PW-treated tamoxifen-resistant cells, but not from control MCF7 cells, in a dose-dependent manner (Fig. 3A and B). MCF7TamR-GFP cells were also engrafted in the presence of single treatments, either tamoxifen alone, or two different concentrations of PW, as above. FACS analysis confirmed a statistically significant reduction in tumour

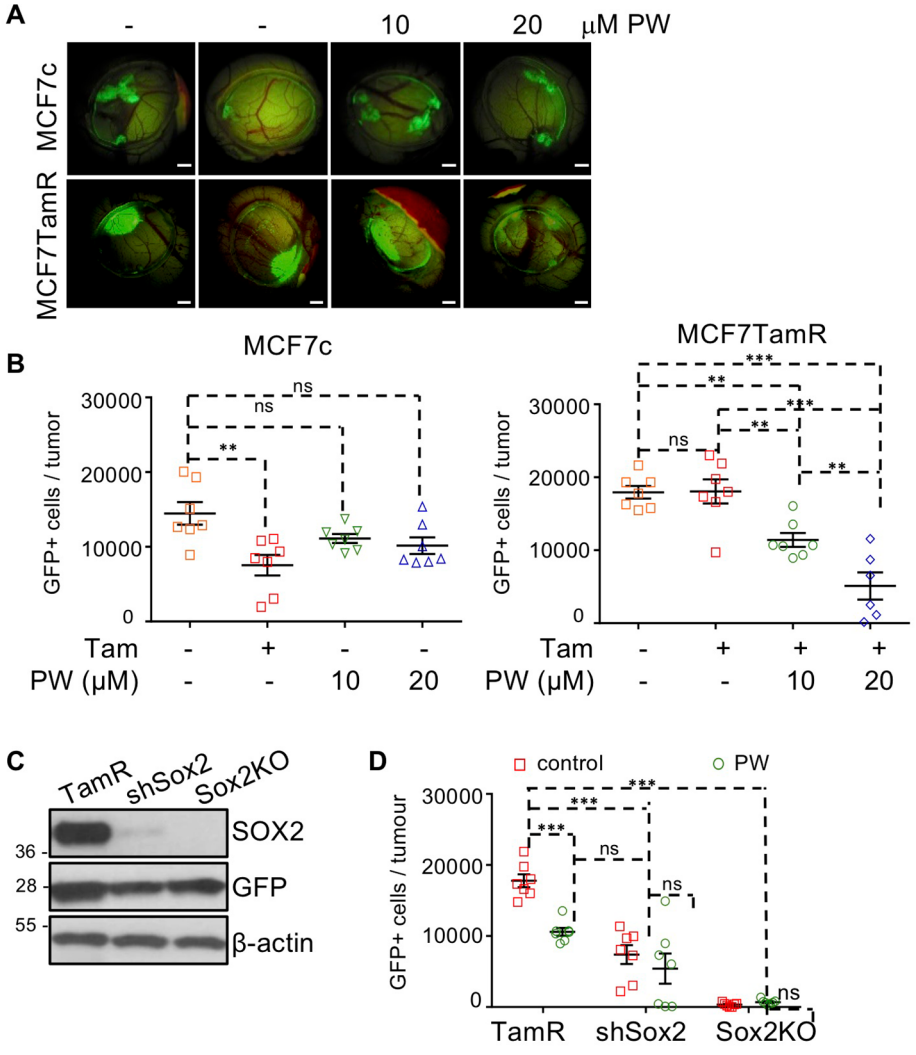

Fig. 3 PW treatment impairs tumorigenesis of tamoxifen-resistant cells in vivo. MCF7c- and MCF7TamR-GFP cells were grafted onto the exposed CAM of chicken embryos at developmental day 7 (EDD7). (**A**) Representative images of tumours formed by MCF7 control or MCF7TamR cells in the CAM. GFP channel (top) and bright-field (down) pictures of the same tumour are shown. (**B**) Quantification of GFP-positive (MCF7c, left; MCF7TamR, right) cells per tumour ($n=7$) in the absence or presence of 5×10^{-7} M tamoxifen and/or 10 or 20 μM PW, using flow cytometry. (**C**) Immunoblot analysis for SOX2, GFP and β-actin (as loading control) proteins in MCF7TamR-GFP (TamR), MCF7TamR-GFP-shSox2 (shSox2) and MCF7TamR-GFP-Sox2KO (Sox2KO) stable cell lines. (**D**) Quantification of GFP-positive cells per tumour ($n=7$) under the different conditions tested (same cell lines as in C and with or without 10 μM PW), using flow cytometry. Scale bar = 1 mm. *p* value: $^{**}p<0.01$

growth in PW-treated tumours (Fig. S3A), although it should be noted that tamoxifen treatment was only absent during the 7 days of the in vivo experiment.

To determine whether the reduction in tumour growth was dependent on the presence of SOX2, we expressed GFP in TamR-shSox2 and TamR-Sox2 KO cells, as above (Fig. 3C). SOX2-silenced MCF7TamR cells formed significantly smaller tumours than control cells, which were similar in size to PW-treated resistant tumours. Crucially, PW treatment did not further reduce the size of tumours formed by SOX2-silenced cells (Fig. 3D, Fig. S3B). TamR- Sox2 KO cells exhibited minimal quantifiable tumour development, reaffirming that SOX2 is essential for tumorigenesis of tamoxifen-resistant breast cancer cells (Fig. 3D). Together, these findings indicate that PW-mediated inhibition of SOX2 impairs tamoxifen-resistant tumour growth in vivo.

Inhibition of SOX2 is responsible for cancer stem cell exhaustion

Next, we wished to establish whether the observed effects of PW on CSCs were due to inhibition of SOX2. Analysis of cells with altered levels of SOX2 (Fig. S4A) showed that secondary mammosphere formation capacity was not affected by PW treatment of SOX2-silenced (shSox2) or -knocked out (Sox2 KO) tamoxifen-resistant cells (Fig. S4B). Moreover, MCF7TamR cells lacking or with reduced levels of SOX2 showed much lower endogenous ALDH activity than tamoxifen-resistant cells, which was not further affected by PW treatment, suggesting that SOX2 expression is also required for the effects of PW on this CSC subpopulation (Fig. 4F).

To assess whether the PW inhibitory effects on the CSC populations were also detected in vivo, we performed extreme limiting dilution analysis (ELDA) [34] in the CAM in vivo model. ELDA assays using MCF7TamR-GFP cells showed that cells treated with PW implanted on the CAM at low density were unable to form substantial tumours, in contrast to untreated cells (Fig. 4G). This assay demonstrated that PW treatment significantly reduced the frequency of tumour-initiating cells by 8.56-fold (p=1.7e-05) in tamoxifen-resistant cells (Fig. S4C). Together, these findings indicate that PW reduces SOX2 activity and exhausts the CSC population (and tumour stemness), leading to reduced tamoxifen resistance in vivo.

PW mechanism of action in tamoxifen-resistant cells

Some POMs have been shown to increase the intracellular levels of reactive oxygen species (ROS), which may lead to apoptosis, in a variety of cell lines [14, 35, 36]. Mitochondrial dysfunction induced by POM species has also been observed in vivo [37, 38]. We found that PW treatment preferentially triggered mitochondrial ROS production in tamoxifen-resistant cells (Fig. 5A, Fig. S5A). Consequently, PW treatment resulted in cleaved PARP protein, leading to reduced levels of the anti-apoptotic protein Bcl-2 (Fig. 5B), and significantly increased the percentage of both early and late apoptotic cells in tamoxifen-resistant cells, but not in control cells or cells lacking SOX2, as assessed by Annexin V staining using FACS (Fig. 5C, D and E and Fig. S5B). Importantly, these findings confirm induction of apoptosis in tamoxifen-resistant cells in response to PW, without significantly affecting parental control breast cancer cells.

Several reports, including our own work, have shown breast stem cells lack or express low levels of ER [39, 40]. Furthermore, we also found an inverse relationship between SOX2 and ER protein expression, leading to reduced ER transcriptional activity in tamoxifen-resistant cells, while SOX2 silencing reversed tamoxifen resistance in different breast cancer cell models [8]. Based on this inverse correlation, we hypothesised that PW-mediated inhibition of SOX2 may lead to enhanced ER activity in those tamoxifen-resistant breast cancer cells that might have survived PW treatment. In fact, it is known that ligand-activated ER represses SOX2 expression [8], thus, we investigated whether SOX2 can regulate ER expression. First, analysis of the promoter sequence of the *ESR1* gene using JASPAR database of transcription factor binding profiles (http://jaspar.genereg.net/) identified a putative SOX2 binding site following the sequence CTTTG TA. Chromatin immunoprecipitation (ChIP) analysis showed that specific SOX2 recruitment at -292 bp of the *ESR1* promoter transcription start site was impaired by PW treatment in MCF7TamR cells (Fig. 6A) and in MCF-7Sox2 overexpressing cells (Fig. 6B), suggesting a direct regulation of ER expression levels by SOX2. Next, PW treatment in ERE-dependent luciferase assays showed increased activation by estrogen in tamoxifen-resistant cells, recovering transcriptional activity to levels found in MCF7c cells (Fig. 6C). This rescue of ER transcriptional activity by PW was also observed in a different model of resistance, ZR75-1TamR cells (Fig. 6D). Furthermore, analysis of ER transcriptional activity under single or combined (tamoxifen and/or PW) treatment conditions in cells with different SOX2 levels suggested that the increased response to estrogen observed in cells treated with PW is strongest in cells with high SOX2 levels of expression (Fig. S6A-C).

Analysis of endogenous ER target genes showed significant estrogen-dependent activation of PS2 in the presence of PW treatment, both at the level of mRNA (Fig. S6D) and protein (Fig. 6E), suggesting the partial recovered activation of ER signalling in tamoxifen-resistant cells. Moreover, tamoxifen-resistant cells lacking SOX2 expression (Fig. 2E) also presented increased PS2 levels in an estrogen-dependent manner, similar to those

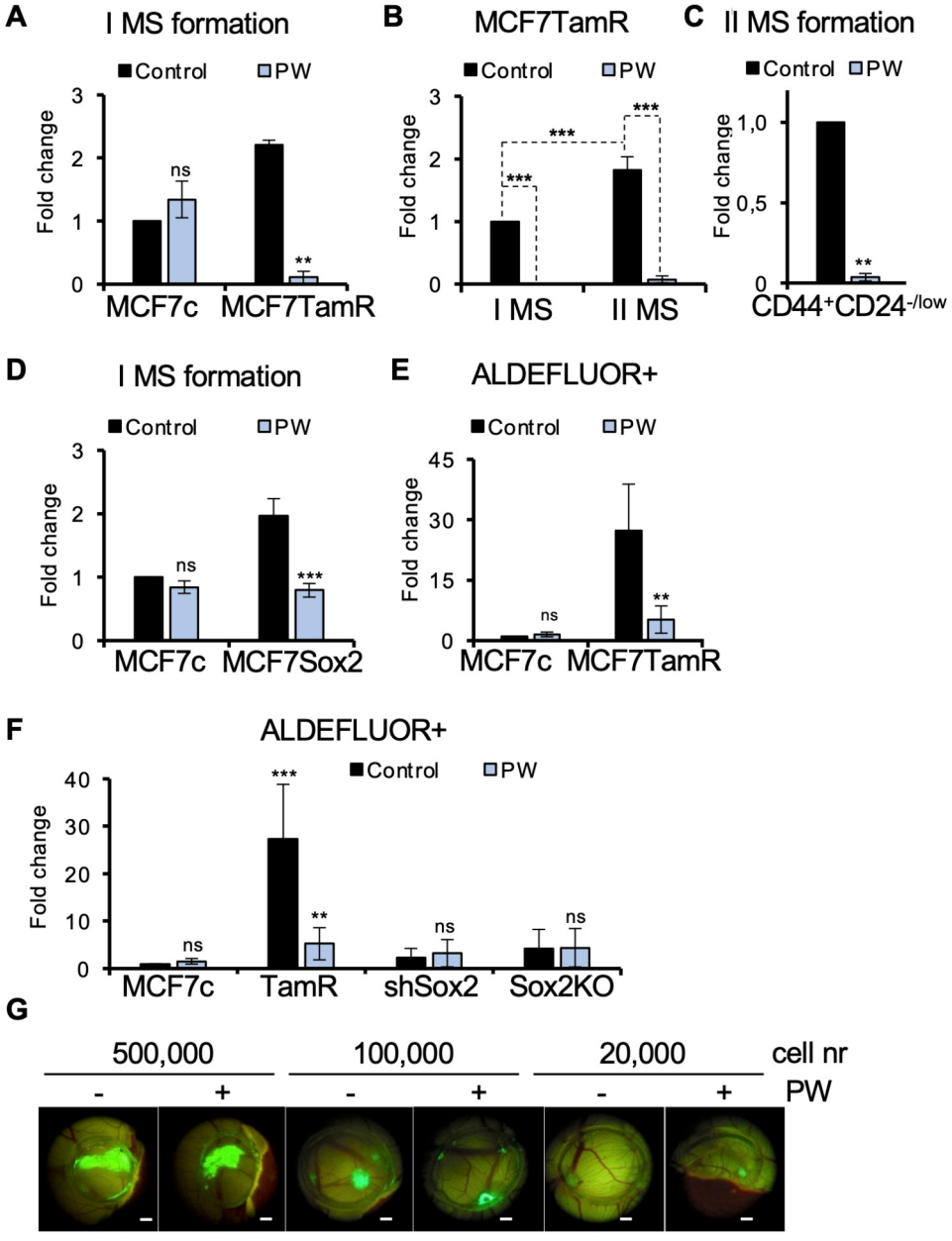

Fig. 4 PW reduces stemness in vitro and in vivo. (**A**) Mammosphere formation of MCF7c and MCF7TamR cells in the absence or presence of 10 μM PW for 5 days. (**B**) Primary (I MS) and secondary mammosphere (II MS) formation assay using MCF7TamR cells with or without 10 μM PW treatment for 5 days. (**C**) Secondary mammosphere formation of $CD44^{+}CD24^{-/low}$ CSCs sorted from MCF7TamR cells treated +/- 10 μM PW for 5 days. (**D**) Mammosphere formation of MCF7c and MCF7Sox2 overexpressing cells in the absence or presence of 10 μM PW for 5 days. (**E**) ALDEFLUOR activity of MCF7c and MCF7TamR cells, quantified by FACS, +/- 10 μM PW for 72 h. (**F**) FACS analysis of ALDEFLUOR positive MCF7c, MCF7TamR, MCF7TamR-shSox2 and MCF7TamR-Sox2KO cells in the absence or presence of 10 μM PW for 72 h. (**G**) Representative bright-field images of tumours formed when different numbers of MCF7TamR-GFP cells (as indicated) were grafted onto the exposed CAM of chicken embryos at developmental day 7 (EDD7) in the presence of 10 μM PW ($n = 7$). Scale bar = 1 mm. *p* value: $^{**}p < 0.01$, were calculated using one-way ANOVA

achieved by PW treated MCF7TamR cells, confirming once again that PW treatment mimics the effect of genetic SOX2 depletion (Fig. 6F). However, the expression levels of other ER target genes, such as amphiregulin (*AREG*), were only partially recovered (Fig. S6E), or not affected, such as growth regulating estrogen receptor binding 1 (*GREB1*) (Fig. S6F), suggesting that there is not a full recovery of ER activity, at least within the conditions tested. Together these findings show that the compromised ER transcriptional activity in tamoxifen-resistant cells is relieved by PW-mediated inhibition of SOX2 activity, leading to partially restored ER signalling pathway activation and hormone sensitivity in tamoxifen-resistant cells, both in vitro and in vivo.

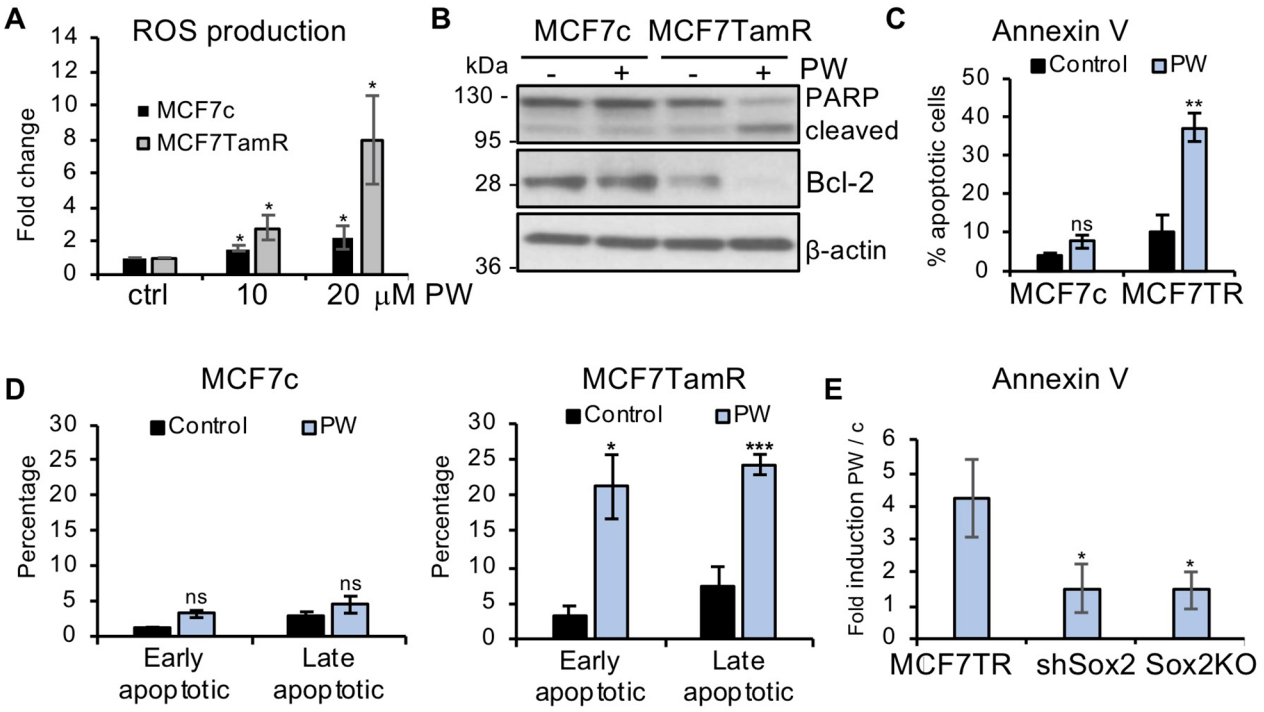

Fig. 5 PW treatment increases apoptosis in tamoxifen-resistant cells. (**A**) Analysis of mitochondrial ROS levels using fluorescent probe MitoSOX in control and resistant cells in the absence or presence of two different PW concentrations (10 and 20 μM) for 48 h ($n=3$). (**B**) Western blot analysis of cleaved PARP and Bcl-2 expression levels in MCF7c and MCF7TamR cells grown in the absence or presence of 10 μM PW. β-actin was used as loading control. (**C**) Quantification of total apoptotic (Annexin V assay) control and resistant cells in response to 10 μM PW for 7 days. (**D**) Graphical representation of the percentage of early and late apoptotic MCF7c (left) and MCF7TamR (right) cells treated with 10 μM PW for 7 days. (**E**) Fold induction of apoptosis in MCF7TamR cells, or resistant cells with reduced (shSox2) or knocked out (Sox2 KO) endogenous SOX2 levels, in response to 10 μM PW for 7 days ($n=4$)

Discussion

CSCs have been shown to employ a variety of mechanisms to resist current forms of therapies, leading to tumour recurrence in many patients [41]. Here we demonstrate that PW, a polyoxometalate, specifically blocks SOX2 binding to DNA response elements. As a consequence, PW reduces cancer cell migration and invasion and impairs tumour formation, leading to stem cell depletion in vivo. Mechanistically, PW induces the formation of reactive oxygen species (ROS) and inhibits Bcl-2 levels, resulting in increased death of tamoxifen-resistant cells. The partially recovered ER transcriptional activity implies that cells are now more sensitive to tamoxifen, thus contributing to the elimination of tamoxifen-resistant cells. These findings show that chemical inhibition of SOX2 by PW recapitulates the effects of SOX2 genetic deletion, including inhibition of cancer stemness and tamoxifen resistance.

SOX2 expression has been shown to be increased in tamoxifen-resistant breast cancer cells, while SOX2 overexpression has been associated with poor survival of breast cancer patients, rendering it an attractive biomarker and therapeutic target [8]. Consequently, a variety of SOX2-targeting approaches have been attempted [42]. For example, blocking SOX2 expression using the neddylation inhibitor MLN4924 has been shown to overcome tamoxifen resistance of breast cancer cells in vitro and in vivo [43]. Another approach, through inhibition of SOX2-DNA interaction, used PIP-S2, a hairpin pyrrole–imidazole polyamides (PIPs)-based bioactive synthetic DNA-binding inhibitor that competes with SOX2 for its consensus target DNA sequence, to guide human induced pluripotent stem cells towards mesoderm differentiation [44]. Here, we have demonstrated that PW interferes with SOX2 binding to specific DNA target sequences, leading to reduced migration and invasion through the down-regulation of SNAI2, one of the key regulators of EMT [45]. Similarly, Wells-Dawson type anions have shown the ability to inhibit the activity of aquaporin-3 (AQP3), when expressed at high levels, and reduce melanoma cell migration [46]. Furthermore, PW significantly reduced the capacity of tamoxifen-resistant cells to form tumours in vivo in a dose-dependent manner, while sparing cancer cells with low or absent SOX2 levels. In addition, PW targeted different subpopulations of CSCs, leading to stem cell depletion and compromised tumour formation, particularly in tamoxifen-resistant cells or cancer cells with high SOX2 levels. Similarly, down-regulation of SOX2 by other means, such as treatment with actinomycin D [47], or through TRPS1-mediated repression [48], were

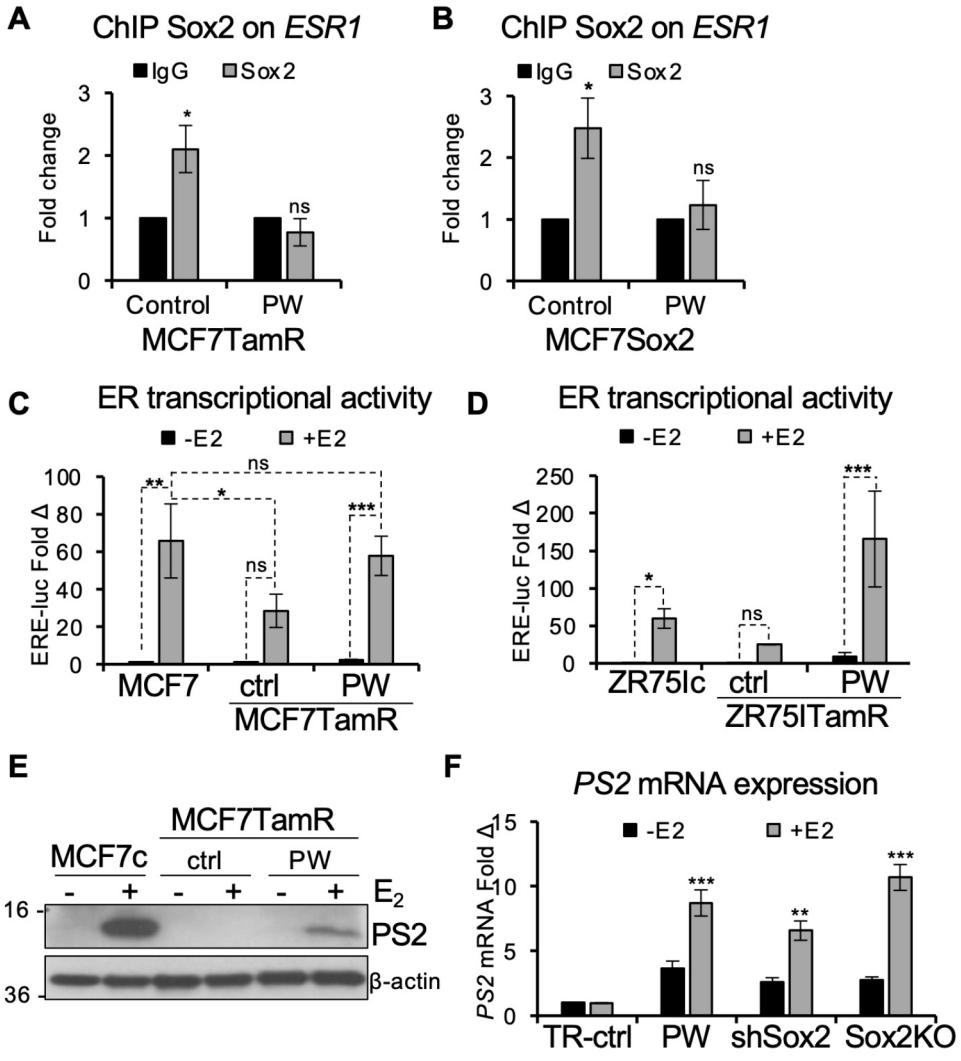

Fig. 6 PW treatment leads to partial recovery of ER transcriptional activity. (**A**) Chromatin immunoprecipitation of SOX2 (or IgG as control) on *ESR1* promoter from MCF7TamR cells in the absence or presence of 10 μM PW. (**B**) As in A, now performing the immunoprecipitation assay using cells overexpressing SOX2, MCF7Sox2 cells treated with PW. (**C**) MCF7c and MCF7TamR cells were transfected with a reporter plasmid containing three copies of a consensus ERE driving a luciferase reporter in the presence of the carrier ethanol (-E2) or 10^{-8} M estrogen (+E2) during 72 h. MCF7TamR cells were, in addition, treated with 10 μM PW, when indicated. β-galactosidase activity was used to control for transfection efficiency and data were normalised to ER activity in MCF7 control cells in the absence of estrogen. (**D**) Transcriptional assays, conditions as in C, performed using ZR75-1c and ZR75-1 tamoxifen-resistant cells. (**E**) PS2 expression in estrogen starved MCF7c and MCF7TamR cells by western blot analysis. Cells were treated with10 μM PW for 72 h, as indicated, in presence of vehicle (ethanol) or 10^{-8} M estrogen. (**F**) *PS2* mRNA expression levels in MCF7TamR cells growing in the presence of tamoxifen as control (ctrl) or with10 μM PW for 72 h, compared to expression in cells with low levels (TamR-shSox2) or lacking (TamR-Sox2KO) SOX2 expression, in the presence of 10 μM PW plus vehicle ethanol (-E2) or 10^{-8} M estrogen (+E2). Graphs represent the mean and standard deviation of three independent experiments. *p* values were calculated using two-way ANOVA tests

also shown to deplete the stem cell population, which abrogated the tumour-initiation capacity of breast cancer cells.

Evasion of cell death is a hallmark of cancer. A variety of POMs have shown anti-apoptotic activity through different mechanisms [14], including decreasing levels of the antiapoptotic protein Bcl-2 [49, 50]. Bcl-2 is often overexpressed in ER-positive breast cancer, which has led to the development of inhibitors that have shown their potential, in combination with CDK4/6 inhibitors, in ER-positive breast cancer [51]. We found that PW induced ROS, leading to reduced Bcl-2 expression and increased apoptosis, suggesting that PW treatment would preferentially target CSCs with high levels of SOX2 expression, resulting in cell death and inability to reinitiate tumour formation in tamoxifen-resistant breast cancer cells.

Importantly, ectopic expression of SOX2 is sufficient to render sensitive cells more resistant to tamoxifen [8], while inhibition of SOX2 activity by PW in

tamoxifen-resistant cells restored their sensitivity to tamoxifen in vivo. These findings mimic the observed effects of tamoxifen on SOX2-depleted tamoxifen-resistant cells, which partially recover ER transcriptional activity, rendering cells sensitive to tamoxifen. Similarly, depletion of SETD1A, a histone H3-lysine 4 methyltransferase that binds to SOX2 and enhances expression of *SOX2* genes in tamoxifen-resistant breast cancer cells, has also been shown to restore their sensitivity to tamoxifen [52]. SOX2 is involved in maintaining stem cells and our findings demonstrate that PW treatment reduces the CSC population, leading to a more differentiated phenotype. The cancer stem cell theory proposes that a small number of CSCs may resist current cancer therapy and regenerate to cause recurrent cancer, which represents a challenge for breast cancer management. Indeed, SOX2 expression is higher in tumours from breast cancer patients who have not responded to tamoxifen therapy [8, 52]. Together, these observations highlight the potential use of PW as a SOX2 inhibitor and the therapeutic relevance of targeting SOX2 to treat tamoxifen-resistant breast cancer. The findings that PW acts preferentially in tamoxifen-resistant cells or cancer cells with high SOX2 levels suggest the existence of a window of opportunity for PW as SOX2 inhibitor. Thus, in a future clinical setting, tumours with high SOX2 expression levels, which can be detected by IHC in clinical samples, as previously reported by our lab [53], would identify patients at high risk of developing resistance to hormone therapy. Consequently, a combination of tamoxifen (to target ER-positive cancer cells) and PW (to target SOX2-positive CSCs) could be used to reduce and or delay development of resistance to tamoxifen in breast cancer patients.

Fulvestrant is a type of hormone therapy that may be used to treat women with locally advanced or metastatic breast cancer or if breast cancer has become resistant to tamoxifen or aromatase inhibitors [54]. Multiple trails have been exploring its potential in combination therapy with other types of drugs and inhibitors, so we tested its potential synergistic effect with PW in tamoxifen resistant cells. Single drug dose-response curves showed that fulvestrant, in contrast to PW (Fig. S7A), only exhibited a minor inhibitory effect on cell proliferation, and this was not dose-dependent (Fig. S7B). Fulvestrant works by degrading ER and tamoxifen-resistant cells are not depending on ER for growth, which may explain this observation. Combinatorial treatment of PW and fulvestrant also led to a decrease in cell viability (Fig. S1C) but it was not synergistic (Fig. S1D). Fulvestrant-resistant MCF7 cells have been previously shown to have increased levels of SOX2 [30]. Here, we performed an acute treatment of fulvestrant in MCF7TamR cells that already have increased SOX2 levels and diminished ER activity, which might explain why PW/fulvestrant combinatorial treatment did not produce any synergistic effect on cell viability in these cells. Although beyond the scope of this manuscript, further functional assays with this treatment combination are warranted.

Importantly, any strategy designed to reduce SOX2 activity should consider observations about the presence of SOX2 in different tissues, including in the healthy human breast [19], although at much lower levels than in tumours [55], which could result in off-target or adverse effects. This possibility emphasises the need to identify suitable concentrations that target preferentially highly SOX2 expressing cells in a specific fashion.

The mechanisms of action responsible for the effects of POMs on different types of carcinomas are still to be deduced and clarified, however, scientific evidence is accumulating about the potential use of such metallodrugs as anticancer therapy in the future [17]. Nevertheless, previously, concerns about the potential toxicity or low bioactivity of POMs have contributed to the development of POM-based nanocomposites [14, 16]. A suitable drug-delivery system can contribute to improve efficiency and selectivity [56], paving the way for POM-based disease therapy, which could also be further tested in additional in vivo models, such as intraductal xenografts [57–59]. Here, our findings illustrate the potential to identify a window of opportunity for PW activity, in this case by interfering with SOX2 DNA binding ability. Thus, this study represents a proof-of-concept of the potential of PW as a therapy against tumour recurrence in breast cancer.

Conclusions

The data in this study confirm the potential for pharmacological inhibition of SOX2 by polyoxometalates as a promising strategy to reduce or eliminate CSCs with high SOX2 levels. The combination of a current hormonal therapy with SOX2 inhibitors, such as PW, may provide a novel strategy to treat breast cancer and reduce or delay the risk of tumour recurrence. Furthermore, these findings warrant additional research to optimise both the activity and selectivity of the treatment, and to enable targeted delivery of the PW anion for effective SOX2 pharmacological inhibition as potential combinatorial therapy with hormone treatments.

Supplementary Information

The online version contains supplementary material available at https://doi.org/10.1186/s12964-024-01800-w.

Supplementary Material 1

Supplementary Material 2

Supplementary Material 3

Supplementary Material 4

Supplementary Material 5

Supplementary Material 6

Supplementary Material 7

Supplementary Material 8

Supplementary Material 9

Acknowledgements
We would like to thank Julia San Millan and other members of the laboratory for help with the CAM assays.

Author contributions
I.A-R and MdM.V. designed and performed experiments, analysed data, created the figures, and wrote the manuscript. S.Y.L., M.R., I.G-C., V.G-A., I.G., I.R., C.P., performed experiments and analysed data. R.M.K., B.A., J.M.G-Z., analysed data and wrote the manuscript. M.dM.V. conceived the idea, supervised the study, analysed data, administered project, sought funding, and wrote the manuscript.

Funding
The authors thank grant support from the Basque Government (IT1722-22 and Elkartek KK-2022/00045) and Spanish Ministry of Science, Innovation and Universities (MICINN, grant PID2022-139530NB-I00) (JMGZ). This research was also funded by Elkartek (KK-2022/00045) by the Basque Government (MdMV), and by the Spanish Ministry of Science and Innovation MCIN/AEI/https://doi.org/10.13039/501100011033 (to MdMV and RK: CEX2021-001136-S; PRE2018-087073 to IG; PID2020-118464RB-I00 to MdMV, and PID2020-117649RB-100 to RK).

Data availability
No datasets were generated or analysed during the current study.

Declarations

Ethics approval and consent to participate
There are no ethics approval required for working with chicken embryos (for CAM assays), according to EU regulations.

Consent for publication
Not applicable.

Competing interests
The authors declare no competing interests.

Received: 30 April 2024 / Accepted: 19 August 2024
Published online: 02 September 2024

References

1. Sung H, Ferlay J, Siegel RL, Laversanne M, Soerjomataram I, Jemal A, Bray F. Global Cancer statistics 2020: GLOBOCAN estimates of incidence and Mortality Worldwide for 36 cancers in 185 countries. CA Cancer J Clin. 2021;71:209–49.
2. Font-Diaz J, Jimenez-Panizo A, Caelles C, Vivanco MD, Perez P, Aranda A, Estebanez-Perpina E, Castrillo A, Ricote M, Valledor AF. Nuclear receptors: lipid and hormone sensors with essential roles in the control of cancer development. Semin Cancer Biol. 2021;73:58–75.
3. Pan H, Gray R, Braybrooke J, Davies C, Taylor C, McGale P, Peto R, Pritchard KI, Bergh J, Dowsett M, et al. 20-Year risks of breast-Cancer recurrence after stopping endocrine therapy at 5 years. N Engl J Med. 2017;377:1836–46.
4. Sorlie T, Perou CM, Tibshirani R, Aas T, Geisler S, Johnsen H, Hastie T, Eisen MB, van de Rijn M, Jeffrey SS, et al. Gene expression patterns of breast carcinomas distinguish tumor subclasses with clinical implications. Proc Natl Acad Sci U S A. 2001;98:10869–74.
5. Martelotto LG, Ng CK, Piscuoglio S, Weigelt B, Reis-Filho JS. Breast cancer intra-tumor heterogeneity. Breast Cancer Res. 2014;16:210.
6. Piggott L, Silva A, Robinson T, Santiago-Gomez A, Simoes BM, Becker M, Fichtner I, Andera L, Young P, Morris C, et al. Acquired Resistance of ER-Positive breast Cancer to Endocrine Treatment confers an adaptive sensitivity to TRAIL through posttranslational downregulation of c-FLIP. Clin Cancer Res. 2018;24:2452–63.
7. Walcher L, Kistenmacher AK, Suo H, Kitte R, Dluczek S, Strauss A, Blaudszun AR, Yevsa T, Fricke S, Kossatz-Boehlert U. Cancer Stem cells-origins and biomarkers: perspectives for targeted personalized therapies. Front Immunol. 2020;11:1280.
8. Piva M, Domenici G, Iriondo O, Rabano M, Simoes BM, Comaills V, Barredo I, Lopez-Ruiz JA, Zabalza I, Kypta R, Vivanco M. Sox2 promotes tamoxifen resistance in breast cancer cells. EMBO Mol Med. 2014;6:66–79.
9. Domenici G, Aurrekoetxea-Rodriguez I, Simoes BM, Rabano M, Lee SY, Millan JS, Comaills V, Oliemuller E, Lopez-Ruiz JA, Zabalza I, et al. A Sox2-Sox9 signalling axis maintains human breast luminal progenitor and breast cancer stem cells. Oncogene. 2019;38:3151–69.
10. Narasimhan K, Pillay S, Bin Ahmad NR, Bikadi Z, Hazai E, Yan L, Kolatkar PR, Pervushin K, Jauch R. Identification of a polyoxometalate inhibitor of the DNA binding activity of Sox2. ACS Chem Biol. 2011;6:573–81.
11. Narasimhan K, Micoine K, Lacote E, Thorimbert S, Cheung E, Hasenknopf B, Jauch R. Exploring the utility of organo-polyoxometalate hybrids to inhibit SOX transcription factors. Cell Regen. 2014;3:10.
12. Bijelic A, Aureliano M, Rompel A. The antibacterial activity of polyoxometalates: structures, antibiotic effects and future perspectives. Chem Commun (Camb). 2018;54:1153–69.
13. Geng J, Li M, Ren J, Wang E, Qu X. Polyoxometalates as inhibitors of the aggregation of amyloid beta peptides associated with Alzheimer's disease. Angew Chem Int Ed Engl. 2011;50:4184–8.
14. Bijelic A, Aureliano M, Rompel A. Polyoxometalates as potential next-generation metallodrugs in the Combat Against Cancer. Angew Chem Int Ed Engl. 2019;58:2980–99.
15. Qi W, Zhang B, Qi Y, Guo S, Tian R, Sun J, Zhao M. The Anti-proliferation activity and mechanism of action of K(12)[V(18)O(42)(H(2)O)]·6H(2)o on breast Cancer cell lines. Molecules 2017, 22.
16. Perez-Alvarez L, Ruiz-Rubio L, Artetxe B, Vivanco MD, Gutierrez-Zorrilla JM, Vilas-Vilela JL. Chitosan nanogels as nanocarriers of polyoxometalates for breast cancer therapies. Carbohydr Polym. 2019;213:159–67.
17. Carvalho F, Aureliano M. Polyoxometalates impact as Anticancer agents. Int J Mol Sci 2023, 24.
18. Geisberger G, Gyenge EB, Hinger D, Bosiger P, Maake C, Patzke GR. Synthesis, characterization and bioimaging of fluorescent labeled polyoxometalates. Dalton Trans. 2013;42:9914–20.
19. Simoes BM, Piva M, Iriondo O, Comaills V, Lopez-Ruiz JA, Zabalza I, Mieza JA, Acinas O, Vivanco MD. Effects of estrogen on the proportion of stem cells in the breast. Breast Cancer Res Treat. 2011;129:23–35.
20. Vivanco MD, Johnson R, Galante PE, Hanahan D, Yamamoto KR. A transition in transcriptional activation by the glucocorticoid and retinoic acid receptors at the tumor stage of dermal fibrosarcoma development. Embo J. 1995;14:2217–28.
21. Oliemuller E, Newman R, Tsang SM, Foo S, Muirhead G, Noor F, Haider S, Aurrekoetxea-Rodriguez I, Vivanco MD, Howard BA. SOX11 promotes epithelial/mesenchymal hybrid state and alters tropism of invasive breast cancer cells. Elife 2020, 9.
22. Romero D, Al-Shareef Z, Gorrono-Etxebarria I, Atkins S, Turrell F, Chhetri J, Bengoa-Vergniory N, Zenzmaier C, Berger P, Waxman J, Kypta R. Dickkopf-3 regulates prostate epithelial cell acinar morphogenesis and prostate cancer cell invasion by limiting TGF-beta-dependent activation of matrix metalloproteases. Carcinogenesis. 2016;37:18–29.
23. Murillo-Garzon V, Gorrono-Etxebarria I, Akerfelt M, Puustinen MC, Sistonen L, Nees M, Carton J, Waxman J, Kypta RM. Frizzled-8 integrates Wnt-11 and transforming growth factor-beta signaling in prostate cancer. Nat Commun. 2018;9:1747.
24. Iriondo O, Rabano M, Domenici G, Carlevaris O, Lopez-Ruiz JA, Zabalza I, Berra E, Vivanco M. Distinct breast cancer stem/progenitor cell populations require either HIF1alpha or loss of PHD3 to expand under hypoxic conditions. Oncotarget. 2015;6:31721–39.

25. Yamase T. Polyoxometalates active against tumors, viruses, and bacteria. Prog Mol Subcell Biol. 2013;54:65–116.
26. Yanagie H, Ogata A, Mitsui S, Hisa T, Yamase T, Eriguchi M. Anticancer activity of polyoxomolybdate. Biomed Pharmacother. 2006;60:349–52.
27. Graham CR, Finke RG. The classic Wells-Dawson polyoxometalate, K6[alpha-P2W18O62].14H2O. Answering an 88 year-old question: what is its preferred, optimum synthesis? Inorg Chem. 2008;47:3679–86.
28. Gumerova NI, Rompel A. Speciation atlas of polyoxometalates in aqueous solutions. Sci Adv. 2023;9:eadi0814.
29. Kim M, Jang K, Miller P, Picon-Ruiz M, Yeasky TM, El-Ashry D, Slingerland JM. VEGFA links self-renewal and metastasis by inducing Sox2 to repress miR-452, driving slug. Oncogene. 2017;36:5199–211.
30. Alves CL, Elias D, Lyng MB, Bak M, Ditzel HJ. SNAI2 upregulation is associated with an aggressive phenotype in fulvestrant-resistant breast cancer cells and is an indicator of poor response to endocrine therapy in estrogen receptor-positive metastatic breast cancer. Breast Cancer Res. 2018;20:60.
31. Deryugina EI, Quigley JP. Chap. 2. Chick embryo chorioallantoic membrane models to quantify angiogenesis induced by inflammatory and tumor cells or purified effector molecules. Methods Enzymol. 2008;444:21–41.
32. Villanueva H, Sikora AG. The Chicken embryo Chorioallantoic membrane (CAM): a Versatile Tool for the study of patient-derived xenografts. Methods Mol Biol. 2022;2471:209–20.
33. Simoes BM, Vivanco MD. Cancer stem cells in the human mammary gland and regulation of their differentiation by estrogen. Future Oncol. 2011;7:995–1006.
34. Hu Y, Smyth GK. ELDA: extreme limiting dilution analysis for comparing depleted and enriched populations in stem cell and other assays. J Immunol Methods. 2009;347:70–8.
35. Leon IE, Porro V, Astrada S, Egusquiza MG, Cabello CI, Bollati-Fogolin M, Etcheverry SB. Polyoxometalates as antitumor agents: Bioactivity of a new polyoxometalate with copper on a human osteosarcoma model. Chem Biol Interact. 2014;222:87–96.
36. Shi G, Jiang H, Yang F, Lin Z, Li M, Guo J, Liao X, Lin Y, Cai X, Li D. NIR-responsive molybdenum (Mo)-based nanoclusters enhance ROS scavenging for osteoarthritis therapy. Pharmacol Res. 2023;192:106768.
37. Soares SS, Gutierrez-Merino C, Aureliano M. Mitochondria as a target for decavanadate toxicity in Sparus aurata heart. Aquat Toxicol. 2007;83:1–9.
38. Aureliano M, De Sousa-Coelho AL, Dolan CC, Roess DA, Crans DC. Biological consequences of Vanadium effects on formation of reactive oxygen species and lipid peroxidation. Int J Mol Sci 2023, 24.
39. Clayton H, Titley I, Vivanco M. Growth and differentiation of progenitor/stem cells derived from the human mammary gland. Exp Cell Res. 2004;297:444–60.
40. Liu S, Ginestier C, Charafe-Jauffret E, Foco H, Kleer CG, Merajver SD, Dontu G, Wicha MS. BRCA1 regulates human mammary stem/progenitor cell fate. Proc Natl Acad Sci U S A. 2008;105:1680–5.
41. Gasch C, Ffrench B, O'Leary JJ, Gallagher MF. Catching moving targets: cancer stem cell hierarchies, therapy-resistance & considerations for clinical intervention. Mol Cancer. 2017;16:43.
42. Zhang S, Xiong X, Sun Y. Functional characterization of SOX2 as an anticancer target. Signal Transduct Target Ther. 2020;5:135.
43. Yin Y, Xie CM, Li H, Tan M, Chen G, Schiff R, Xiong X, Sun Y. The FBXW2-MSX2-SOX2 axis regulates stem cell property and drug resistance of cancer cells. Proc Natl Acad Sci U S A. 2019;116:20528–38.
44. Taniguchi J, Pandian GN, Hidaka T, Hashiya K, Bando T, Kim KK, Sugiyama H. A synthetic DNA-binding inhibitor of SOX2 guides human induced pluripotent stem cells to differentiate into mesoderm. Nucleic Acids Res. 2017;45:9219–28.
45. Di-Cicco A, Petit V, Chiche A, Bresson L, Romagnoli M, Orian-Rousseau V, Vivanco M, Medina D, Faraldo MM, Glukhova MA, Deugnier MA. Paracrine met signaling triggers epithelial-mesenchymal transition in mammary luminal progenitors, affecting their fate. Elife 2015, 4.
46. Pimpao C, da Silva IV, Mosca AF, Pinho JO, Gaspar MM, Gumerova NI, Rompel A, Aureliano M, Soveral G. The aquaporin-3-Inhibiting potential of Polyoxotungstates. Int J Mol Sci 2020, 21.
47. Das T, Nair RR, Green R, Padhee S, Howell M, Banerjee J, Mohapatra SS, Mohapatra S. Actinomycin D down-regulates SOX2 expression and induces death in breast Cancer stem cells. Anticancer Res. 2017;37:1655–63.
48. Gong X, Liu W, Wu L, Ma Z, Wang Y, Yu S, Zhang J, Xie H, Wei G, Ma F, et al. Transcriptional repressor GATA binding 1-mediated repression of SRY-box 2 expression suppresses cancer stem cell functions and tumor initiation. J Biol Chem. 2018;293:18646–54.
49. Wang L, Zhou BB, Yu K, Su ZH, Gao S, Chu LL, Liu JR, Yang GY. Novel antitumor agent, trilacunary keggin-type tungstobismuthate, inhibits proliferation and induces apoptosis in human gastric cancer SGC-7901 cells. Inorg Chem. 2013;52:5119–27.
50. Wang L, Yu K, Zhu J, Zhou BB, Liu JR, Yang GY. Inhibitory effects of different substituted transition metal-based krebs-type sandwich structures on human hepatocellular carcinoma cells. Dalton Trans. 2017;46:2874–83.
51. Whittle JR, Vaillant F, Surgenor E, Policheni AN, Giner G, Capaldo BD, Chen HR, Liu HK, Dekkers JF, Sachs N, et al. Dual targeting of CDK4/6 and BCL2 pathways augments Tumor Response in Estrogen receptor-positive breast Cancer. Clin Cancer Res. 2020;26:4120–34.
52. Jin ML, Yang L, Jeong KW. SETD1A-SOX2 axis is involved in tamoxifen resistance in estrogen receptor alpha-positive breast cancer cells. Theranostics. 2022;12:5761–75.
53. Piva M, Domenici G, Iriondo O, Rabano M, Simoes BM, Comaills V, Barredo I, Lopez-Ruiz JA, Zabalza I, Kypta R, Vivanco MDM. Sox2 promotes tamoxifen resistance in breast cancer cells. EMBO Mol Med. 2014;6:66–79.
54. Nathan MR, Schmid P. A review of fulvestrant in breast Cancer. Oncol Ther. 2017;5:17–29.
55. Rodriguez-Pinilla SM, Sarrio D, Moreno-Bueno G, Rodriguez-Gil Y, Martinez MA, Hernandez L, Hardisson D, Reis-Filho JS, Palacios J. Sox2: a possible driver of the basal-like phenotype in sporadic breast cancer. Mod Pathol. 2007;20:474–81.
56. Zhao H, Zhao C, Liu Z, Yi J, Liu X, Ren J, Qu X. A polyoxometalate-based pathologically activated assay for efficient Bioorthogonal Catalytic Selective Therapy. Angew Chem Int Ed Engl. 2023;62:e202303989.
57. Sflomos G, Dormoy V, Metsalu T, Jeitziner R, Battista L, Scabia V, Raffoul W, Delaloye JF, Treboux A, Fiche M, et al. A preclinical model for ERalpha-Positive breast Cancer points to the epithelial microenvironment as determinant of Luminal phenotype and hormone response. Cancer Cell. 2016;29:407–22.
58. Richard E, Grellety T, Velasco V, MacGrogan G, Bonnefoi H, Iggo R. The mammary ducts create a favourable microenvironment for xenografting of luminal and molecular apocrine breast tumours. J Pathol. 2016;240:256–61.
59. Aouad P, Zhang Y, De Martino F, Stibolt C, Ali S, Ambrosini G, Mani SA, Maggs K, Quinn HM, Sflomos G, Brisken C. Epithelial-mesenchymal plasticity determines estrogen receptor positive breast cancer dormancy and epithelial reconversion drives recurrence. Nat Commun. 2022;13:4975.

Publisher's note